Molecular Cancer Therapeutics

Preclinical Studies on the Mechanism of Action and the Anti-Lymphoma Activity of the Novel Anti-CD20 Antibody GA101

Stephane Dalle[1,2], Lina Reslan[1], Timothee Besseyre de Horts[1], Stephanie Herveau[1], Frank Herting[3], Adriana Plesa[2], Thomas Friess[3], Pablo Umana[4], Christian Klein[3], and Charles Dumontet[1,2]

Abstract

GA101 is a novel glycoengineered Type II CD20 monoclonal antibody. When compared with rituximab, it mediates less complement-dependent cytotoxicity (CDC). As expected for a Type II antibody, GA101 appears not to act through CDC and is more potent than the Type I antibody rituximab in inducing cell death via nonclassical induction of apoptosis cytotoxicity, with more direct cytotoxicity and more antibody-dependent cell-mediated cytotoxicity. We evaluated the antitumor activity of GA101 against the human-transformed follicular lymphoma RL model *in vivo* in severe combined immunodeficient mice (SCID) mice. GA101 induced stronger inhibition of tumor growth than rituximab. Combination of GA101 with cyclophosphamide *in vivo* confirmed the superiority of GA101 over rituximab. Neutralizing the complement system with cobra venom factor partially impaired the antitumor activity of rituximab, but had no impact on the efficacy of GA101. *In vitro* GA101 more potently induced cell death of RL cells than rituximab. The expression of a limited number of genes was found to be induced by both antibodies after exposure *in vitro*. Among these, early growth response 1 and activation transcription factor 3 were confirmed to be increased at the protein level, suggesting a possible role of these proteins in the apoptotic signalling of anti-CD20 antibodies. These data imply that GA101 is superior to rituximab not only as a single agent, but also in combination with chemotherapy. These data suggest the presence of novel signalization pathways activated after exposure to anti-CD20 antibodies. *Mol Cancer Ther; 10(1); 178–85. ©2011 AACR.*

Introduction

Rituximab, directed against the CD20 antigen on B cells, was the first commercially available monoclonal antibody (mAb) for the treatment of lymphoma. It is the current treatment of choice for a variety of lymphoproliferative disorders including low and high grade B-cell non-Hodgkin's lymphomas (NHL; refs 1–5). Follicular lymphoma (FL) is the most common subtype of indolent lymphoma. Rituximab is now widely used either alone or in combination with multi-agent chemotherapy for the treatment of FL, either at diagnosis (6, 7), at relapse (8–10), or for maintenance therapy (2, 11, 12). However, despite its well-established clinical efficacy, a subpopulation of patients does not initially respond to rituximab and most patients will relapse after rituximab therapy (13, 14). Thus, there is still a need either for more efficient rituximab combination therapies or for novel CD20-specific monoclonal antibodies with increased efficacy (15).

Various *in vitro* and *in vivo* experiments have shown that elimination of CD20+ lymphoma cells by rituximab involves complement-dependent cytotoxicity (CDC; refs 16–23), direct induction of apoptotic signalling (24–26), as well as the recruitment of effector cells leading to antibody-dependent cell-mediated cytotoxicity (27). Nevertheless, the *in vivo* mechanism of action of and resistance to rituximab are not fully understood (28). Depending on their ability to redistribute CD20 into lipid rafts and to induce CDC, or to induce cell death and homotypic adhesion, anti-CD20 mAb can be classified as Type I or II CD20 antibodies. Schematically, Type I antibodies (such as rituximab) induce CDC with redistribution of CD20 into lipid rafts, whereas type II mAB (such as the murine antibody tositumomab, or the humanized antibody GA101) are believed to act primarily through the direct induction of nonclassical cell death and exhibit low CDC activity (29).

Authors' Affiliations: [1]Université de Lyon and INSERM, U590; [2]Hospices Civils de Lyon, Lyon, France; [3]Discovery Oncology, Pharma Research, Roche Diagnostics GmbH, Penzberg, Germany; and [4]GlycArt Biotechnology AG, Schlieren, Switzerland

Note: Supplementary material for this article is available at Molecular Cancer Therapeutics Online (http://mct.aacrjournals.org/).

Corresponding Author: Charles Dumontet, INSERM U590, Laboratoire de Cytologie Analytique, Faculte de Medecine Rockefeller, Universite Claude Bernard Lyon I, Lyon, France. Phone: +33478777236; Fax: +33472119505. Email: charles.dumontet@chu-lyon.fr

doi: 10.1158/1535-7163.MCT-10-0385

Rituximab as a chimeric mAb belongs to the first generation of CD20 antibodies recognizing a Type I epitope. While the second generation of humanized (ocrelizumab, veltuzumab, AME-133, Immu-106) or fully human (ofatumumab) anti-CD20 antibodies recognize a Type I epitope, GA101 represents a novel generation that in addition to being humanized recognizes a type II epitope and is glycoengineered using GlycoMAb technology leading to bisected, afucosylated fragment crystallizable (Fc) region carbohydrates resulting in enhanced affinity for the human FcγRIIIa receptor on human effector cells such as NK cells, macrophages, and dendritic cells (29). GA101 was obtained by grafting CDR sequences from the murine mAB B-ly1 on framework regions with fully human IgG1-kappa germline sequences.

In this study, we compared the effect of GA101 and rituximab on the human follicular RL lymphoma model, both *in vitro* and *in vivo*.

Materials and Methods

Cell lines and culture

The RL cell line, derived from a human transformed FL sample, was purchased from American Type Culture Collection within the 6 months before experimentation and routinely characterized before and during the experimentation regarding the CD19; CD20; HLA DQ, and HLA DR expression. Cells were maintained in culture medium consisting of RPMI-1640 (Life Technologies), 10% of fetal calf serum (Integro), 100 units/mL of penicillin and 100 μg/mL of streptomycin (Life Technologies). All cells were cultured at 37°C in a 5% CO_2 atmosphere.

In vivo studies

Six-week-old female CB17 severe combined immunodeficient mice (SCID) mice purchased from Charles River laboratories (l'Arbresle) were bred under pathogen-free conditions at the animal facility of our institute. Animals were treated in accordance with the European Union guidelines and French laws for the laboratory animal care and use. The animals were kept in conventional housing. Access to food and water was not restricted. This study was approved by the local animal ethical committee.

For xenograft experiments, 1×10^6 RL cells were injected subcutaneously on day 1. Mice were randomized when a tumor became palpable in groups of 10 and treatment was initiated. In a first set of experiments, rituximab and GA101 were used as monotherapy at different dosages twice weekly. The 5 different groups of 10 mice were: control group receiving vehicle (NaCl 0.9%), rituximab (30 mg/kg), GA101 (10 mg/kg), GA101 (30 mg/kg), and GA101 (100 mg/kg). The treatment was administered intravenously twice a week. The mice were closely monitored regarding weight and general status. In experiments evaluating the role of CDC in rituximab inhibition of tumor growth in groups of 3 mice, complement inhibition was induced by weekly intraperitoneal injection of cobra venom factor (CVF; 2 μg/mouse, Quidel Corporation).

Combination studies were done with cyclophosphamide. In these combination studies, the treatment was administrated weekly. The control group received vehicle (NaCl 0.9%), whereas the treated groups received rituximab (30 mg/kg), GA101 (30 mg/kg), rituximab (30 mg/kg) + GA101 (30 mg/kg), cyclophosphamide (50 mg/kg), rituximab + cyclophosphamide (50 mg/kg), and GA101 + cyclophosphamide (50 mg/kg). Rituximab and GA101 (30 mg/kg) were provided by Roche, whereas cyclophosphamide was obtained from Baxter. The mice were injected intravenously in the tail vein, once a week. They were weighed and the tumor size was measured twice a week with an electronic calliper. The tumor volume (*TV*) was estimated from two dimensional tumor measurements by the formula: tumor volume (mm^3) = length (mm) × width^2/2. Median tumor growth inhibition (% TGI) was calculated according to the NCI formula: $1 - ([TV_{\text{treated}}\ (\text{day } 34 - 20) \times 100/TV_{\text{control}}\ (\text{day } 34 - 20) \times 100])$.

Flow cytometry analysis

Cell surface antigen expression of RL cells was performed on a FACS Calibur flow cytometer (Becton Dickinson). Analysis of the data was done with the Cell Quest software program (Becton Dickinson). Mouse fluorochrome-conjugated isotype control antibodies, phycocyanin 5 (PC5)-coupled anti-CD19, phycoerythrin coupled APC anti-CD20, fluorescein isothiocyanate (FITC)-coupled anti-CD59, and PE-coupled anti-CD55 were purchased from Immunotech. FITC-coupled anti-CD46 and FITC active caspase-3 apoptosis kit were purchased from Becton Dickinson. Mean fluorescence intensity (MFI) was determined by subtracting the signal of isotype-matched antibody staining from the staining observed with the specific primary antibody. RL exposed to rituximab, GA 101 and CVF were firstly evaluated *in vitro*, but were also evaluated *ex vivo*, immediately after the extraction of tumor cells from animals. These experiments were done after exposure of 50,000 cells in 6-well culture plates in 2 mL of complete medium to rituximab or GA101 with or without CVF. These assays were done after 1, 2, 4, 6, and 24 hours of culture.

Annexin V/Propidium iodide staining

To evaluate the induction of apoptosis and the reduction of cell viability in cells exposed to antibodies with or without CVF, 10^6 cells were resuspended in 300 μL of human serum and 700 μL of culture medium with or without 100 μg/mL rituximab at 37°C for 6, 15, and 24 hours. Dead and viable cells were discriminated by Annexin V/propidium iodide (PI) staining using flow cytometry. Briefly, the cells were washed and resuspended in binding buffer [10 mmol/L HEPES (pH 7.4), 140 mmol/L NaCl, and 2.5 mmol/L $CaCl_2$] containing 1 mg/mL FITC-Annexin V PI (1.25 mg/mL) was also

added to the samples to distinguish between early apoptosis and secondary necrosis.

Western blot protein analysis

Protein expression was determined by Western blot analysis in rituximab-naive and rituximab-resistant tumors as previously described (30). Briefly, cell lysates were resolved by 12% SDS-PAGE, and transferred onto a polyvinylidene difluoride (PVDF) membrane (Hybond-ECL). The blots were then incubated with the appropriate dilution of primary antibody, followed by incubation with peroxidase-conjugated secondary antibody. For this analysis, 10^7 cells were pelleted and proteins fractionated by SDS-PAGE (12–15% gradient gels) and transferred to a PVDF membrane using an electroblotting apparatus (Bio-Rad). The loading of equal amounts of protein was verified by Ponceau staining of the PVDF membranes. The membrane was blocked with 5% nonfat, dry milk for 1 hour and subsequently incubated with the primary antibody at a dilution of 1:1,000 for 1 hour at room temperature. Antibody directed against Bcl2 was purchased from Dako (clone 124), YY1 from Active Motif, and Bcl-x_L (clone S18) from Santa Cruz; BAX from Santa Cruz (clone SC 493), BAK from Santa Cruz (clone SC 7873), BIM from Santa Cruz (clone SC 8265), CD59 from Serotec (Clone mem-43), CD55 from Abcam (MEM-118), CD20 from Abcam (clone L26), early growth response 1 (EGR1) and activation transcription factor 3 (ATF3) from Santa Cruz, and caspase-3 from BD Biosciences (clone CPP32). Unbound antibody was removed by washing with phosphate buffered saline (pH 7.2) containing 0.1% Tween 20 and 5% nonfat, dry milk. The membrane was then incubated with the secondary antibody (anti mouse peroxydase-conjugated antibody [Sigma] at a dilution of 1:6,000) for 1 hour at room temperature. After extensive washing with phosphate buffered saline, proteins were detected after addition of the staining substrates ECL (Amersham). The proteins were detected by chemiluminescence using Kodak film (Eastman Kodak Company) or using the Odyssey infrared system (LI-COR Biotechnology). The Western blot analyses were done for each animal from the different groups of animals.

Gene expression profiling

To determine which genes were differentially expressed in cells exposed to rituximab or GA101, RL cells were exposed *in vitro* and *in vivo* to these antibodies then analysed by pangenomic profiling using Agilent 44K chips in the Laboratoire de Caractérisation Moléculaire des Tumeurs (LCMT). Briefly, 1-color labeled cRNAs were generated from 200 ng of total RNA using the Low RNA Input Amplification Kit (Agilent Technologies) according to the instructions of the manufacturer. Labeled cRNA were hybridized overnight to Whole Human Genome 4 × 44K microarrays (ref Agilent G4112F) containing 45,015 features representing 41,000 genes. Each probe is a 60-mer, synthesized *in situ*. After washing, microarrays were scanned using the Agilent model G2505B microarray scanner, and data were extracted by Feature Extraction software, version 9.5. The default settings, as 2 photomultiplicator values (XDR high 100% and XDR low 10%), were used to scan the microarrays. Data were normalized using the quantile normalization method (31). Each sample was done in triplicate. Analyses of differentially expressed genes and Gene Ontology pathways (Gene Ontology Consortium, 2000, http://www.geneontology.org/) were done using GeneSpring 7.0. Determination of differentially expressed genes was done using a parametric test, with a false discovery rate of 0.01. Quantitative RT-PCR confirmation of selected genes was done as previously described (30).

Statistical analysis

For the evaluation of tumor growth, calculations started at staging (day 34) until termination for the control group and the group receiving therapy. Values were documented as medians and standard deviations (SD). Median (%) TGI for volume (T/C) was calculated according to the NCI formula:1 - ([TV_treated (day Y − 100/ TV_control (day X − 34) × 100])

Briefly, in a randomized 2-sample design the treatment-to-control ratio:

$$\mathrm{TCR} = \frac{\bar{V}_{\mathrm{treated}}}{\bar{V}_{\mathrm{Control}}}$$

and its 2-sided nonparametric (1-α) confidence interval according to Fieller (1954)/Hothorn and Munzel (2000) were estimated. The calculations were done with the special SAS program TUMGRO (version 3) using version 8.1 (SAS Inc. Cary, 2000).

Results

Inhibition of tumor growth *in vivo* by rituximab or GA101

The efficacy of GA101 and rituximab was compared in the RL model that we recently described (30). In the first study GA101 was administered i.v. twice weekly at 3 dosages (10, 30, and 100 mg/kg), whereas rituximab was given at fixed dose of 30 mg/kg twice weekly (Fig. 1). Both antibodies were administered as intravenous injections, for a total of 5 injections. As shown in Figure 1, we observed that the new CD20 antibody GA101 was more active than rituximab administered at similar doses on established RL tumors. The antitumor effect of GA101 against RL xenografts was dose dependent in terms of TGI. TGI was calculated using NCI formula at day 34 and showed values of 25, 75, and 85% for the 10, 30, and 100 mg/kg dosages of GA101, respectively, whereas the 30 mg/kg dose of rituximab induced a TGI of 43%. The higher doses of 30 and 100 mg/kg of GA101 significantly inhibited the growth of RL tumors and resulted in some complete tumor remissions (10% and 30%, respectively), whereas no complete tumor remissions were observed in the rituximab group. Taken together, the antitumor

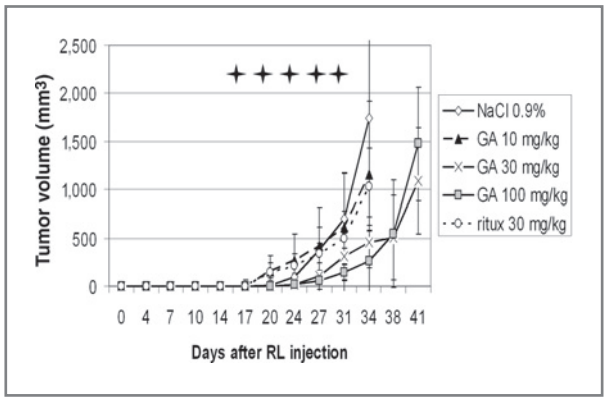

Figure 1. Inhibition of tumor growth *in vivo* by rituximab or GA101. Mice injected with RL cells subcutaneously were treated by IV infusion twice a week starting on day 17 and ending on day 31 (black crosses). The tumors were measured twice a week. The mice were euthanized when the tumor volume reached 2 cm^3. The difference between GA (30 mg/kg) and rituximab (30 mg/kg) was significant ($P = 8.10^{-5}$)

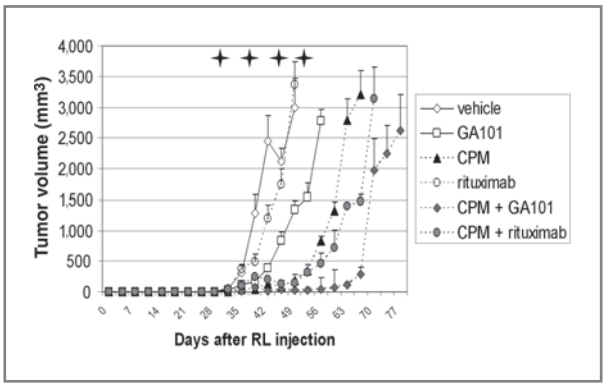

Figure 2. Effect of combination therapy of GA101 or rituximab with cyclophosphamide. Mice-bearing established SC RL tumors were treated weekly (on days 31, 38, 45 and 52 (black crosses). The control group received vehicle (NaCl 0.9%), whereas the treated groups received one of the following: rituximab (30 mg/kg), GA101 (30 mg/kg), rituximab (30 mg/kg) + GA101 (30 mg/kg), cyclophosphamide (CPM; 50 mg/kg), rituximab + CPM (50 mg/kg), GA101 + CPM (50 mg/kg). The difference between rituximab + CPM and GA101 + CPM was significant ($P = 0.05$)

activity of rituximab against RL xenografts was inferior to an equivalent dosing of GA101. Tolerability of GA101 with these regimens was excellent and no significant modification of body weight was observed. Since there was no significant difference between the 30 mg/kg and 100 mg/kg doses of GA101, the 30 mg/kg was used for subsequent combination studies.

Combination of cyclophosphamide with rituximab or GA101 *in vivo*

In a separate series of experiments, rituximab 30 mg/kg and GA101 30 mg/kg were administered once weekly i.v. for 4 weeks, either with or without cyclophosphamide 50 mg/kg administered once weekly i.p. for 4 weeks. As shown in Figure 2, this study confirmed the previous finding that the new anti-CD20 antibody GA101 was more active against established RL tumors than rituximab administered at similar doses. TGI values at day 42 were 79% for GA101, 35% for rituximab, and 93% for cyclophosphamide administered as single agents when compared with untreated controls. When groups receiving combination therapy were compared with the groups receiving the corresponding single agent antibody, cyclophosphamide increased antitumor efficacy with TGI values of 83% at day 42 and 55% at day 66% for rituximab and 94% at day 42 and 88% at day 66 for GA101, respectively. Taken together, the GA101-cyclophosphamide combination was significantly better than the rituximab-cyclophosphamide combination in this setting. Thus, when using a suboptimal dose of the classical antilymphoma alkylating agent cyclophosphamide, the combination of either antibody with cyclophosphamide was more active than either agent alone, and the most active combination was GA101 in combination with cyclophosphamide. In all cases, the administration was well tolerated with no toxic deaths, nor loss of body weight greater than 10% (data not shown).

Role of complement in the antitumor effect of antibodies *in vivo*

Complement-dependent cytotoxicity appears to play a key role in the efficacy of rituximab in the RL model (30). When GA101 or rituximab were administered in combination with CVF, we observed a significant loss of antitumor activity in the rituximab group, whereas we did not observe a loss of efficacy in the GA101 group (Fig. 3). No difference was observed between the rituximab and GA101 groups, we assumed that it was induced by the small number of mice in each group in these experiments. When RL cells were exposed to rituximab or GA101 *in vitro*, the addition of 30% human serum as a source of complement increased the apoptotic fraction in the case of rituximab but not in the case of GA101 (data not shown), thus supporting the lack of CDC in the case of GA101-mediated cytotoxicity.

Flow cytometry and Western blot analyses of tumor cells exposed to antibodies *in vitro* and *in vivo*

To assess the direct effect of GA101 on RL cells, we did PI/Annexin testing. We observed more apoptotic cells (early and late apoptosis) in cells *in vitro* exposed to GA101 than in cells exposed to rituximab. This difference was seen after time exposure varying from 6 to 24 hours (Fig. 4), and disappeared after 48 and 72 hours (data not shown). For instance apoptotic cells (early and late apoptosis) represented 6.70%, 10.72%, 17.35%, respectively, in untreated and rituximab- and GA101-treated cells after 15 hours of exposure to the treatment. As a consequence, the percentage of live cells was more strongly reduced in the GA101 group compared with the rituximab group (Fig. 4). In agreement with this, procaspase-3 protein was

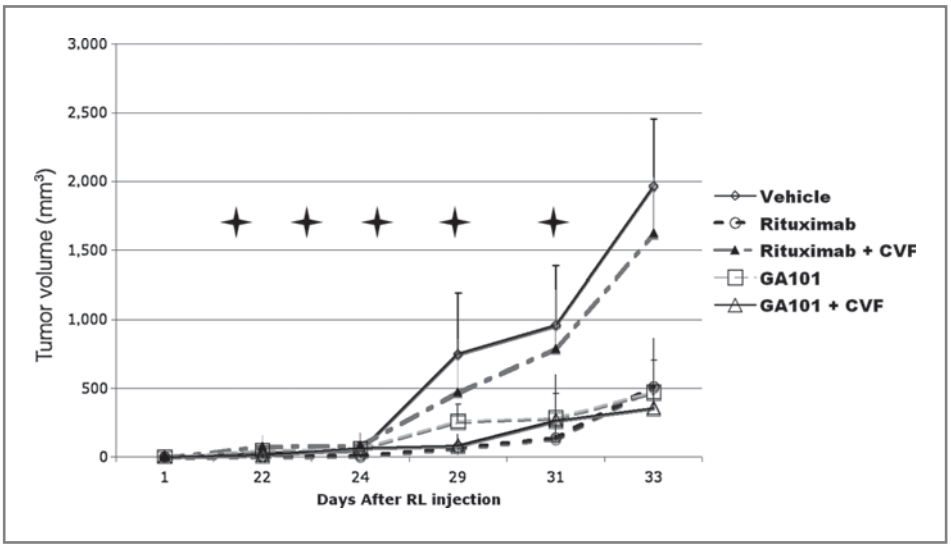

Figure 3. Effect of CVF on the *in vivo* antitumor efficacy of antibodies. The mice (3 animals per group) were treated by IV infusion two times a week starting on day 17 with rituximab (30 mg/kg) and GA101 (30 mg/kg) with or without weekly injection of CVF (2 μg/mouse). The difference between rituximab and rituximab + CVF was significant ($P < 0.05$), whereas the difference between GA101 and GA101 + CVF was not statistically significant.

found to be more strongly expressed in cells exposed to GA101 than in cells exposed to rituximab from 6 hours after the treatment start (data not shown). Although cleaved form of caspase-3 was not detected in the early phase (6 hours), it became detectable on FACS analysis from 12 to 48 hours after exposure (Fig. 5). There were no differences concerning Bim, Bak, Bcl2, Bcl-x_L, caspase-8, and caspase-9 by western-blot analysis and CD20

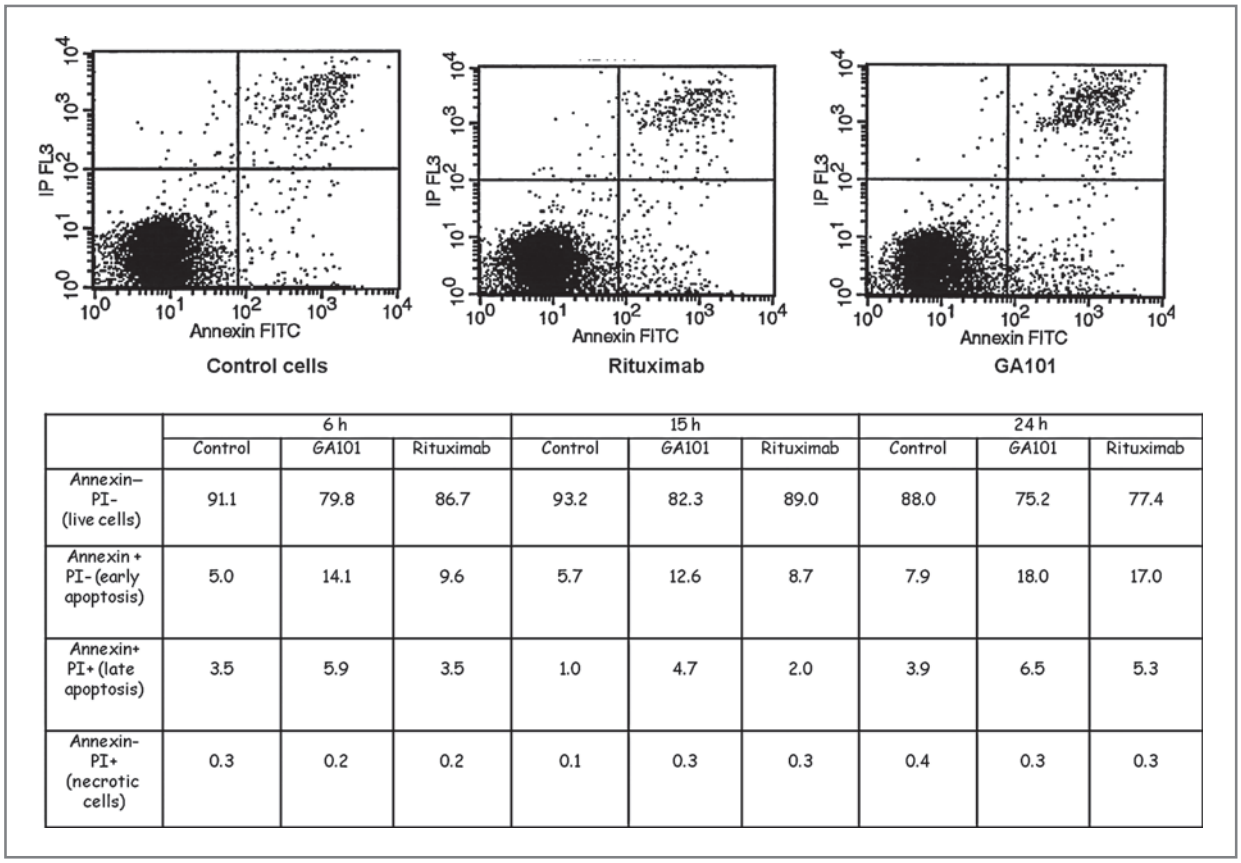

	6 h			15 h			24 h		
	Control	GA101	Rituximab	Control	GA101	Rituximab	Control	GA101	Rituximab
Annexin− PI− (live cells)	91.1	79.8	86.7	93.2	82.3	89.0	88.0	75.2	77.4
Annexin + PI− (early apoptosis)	5.0	14.1	9.6	5.7	12.6	8.7	7.9	18.0	17.0
Annexin+ PI+ (late apoptosis)	3.5	5.9	3.5	1.0	4.7	2.0	3.9	6.5	5.3
Annexin− PI+ (necrotic cells)	0.3	0.2	0.2	0.1	0.3	0.3	0.4	0.3	0.3

Figure 4. Induction of apoptosis by rituximab and GA101 on RL cells. Induction of apoptosis by rituximab and GA101 on RL cells was evaluated by flow cytometry. Apoptosis was evaluated at various time points after exposure to rituximab or GA101 followed by staining with Annexin V and PI. The dot plots represent the PI and Annexin V expression for untreated and rituximab- and GA101-treated cells after 15 hours of *in vitro* exposure. The table shows the results observed in each groups (alive, early, and late apoptotic, necrotic cells) in percentage of 10,000 analyzed cells per condition.

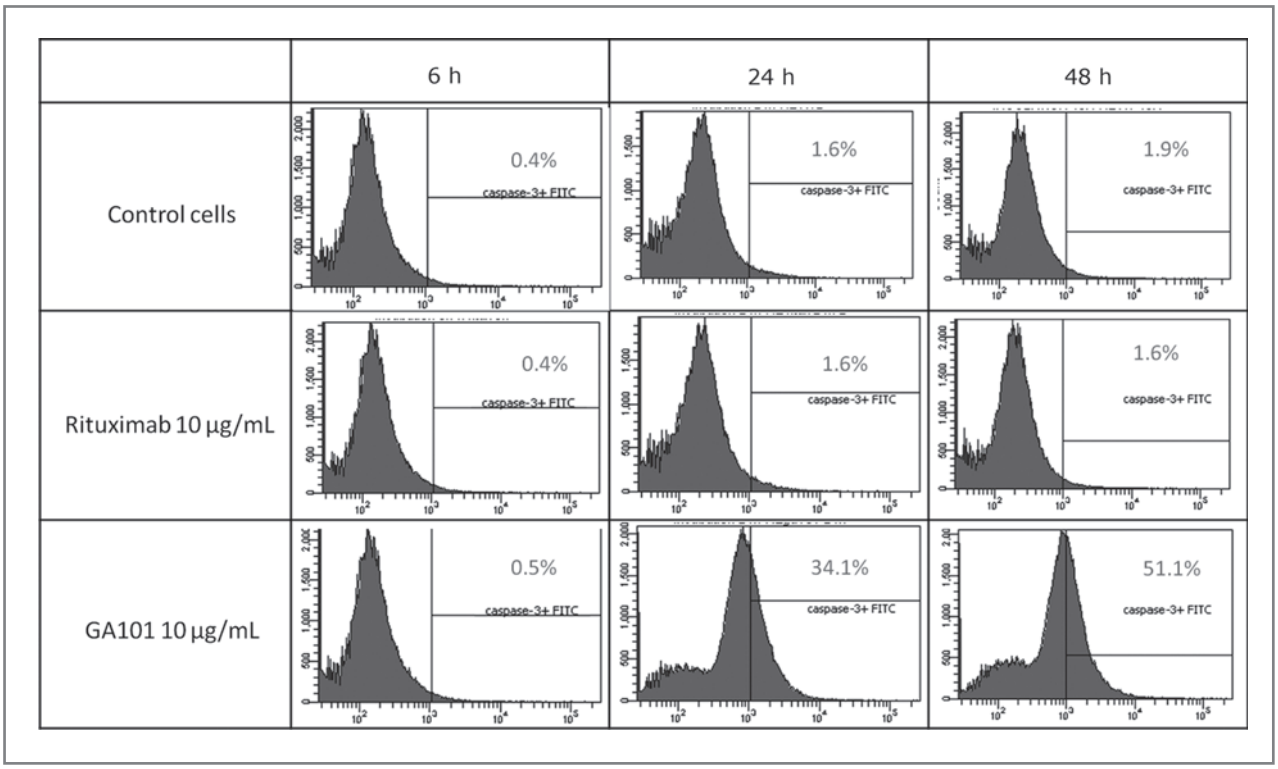

Figure 5. Effect of rituximab and GA101 on caspase-3 expression in RL cells *in vitro*. Cleaved caspase-3 expression was evaluated *in vitro* by FACS analysis after 6, 24, and 48 hours of exposure to either GA101 or rituximab. Percentage represents the number of positive cells.

expression both by FACS and Western blot analysis (data not shown). When cells were co-incubated with antibodies and CVF, the quantities of caspase-3 appeared to be decreased in the case of rituximab-exposed cells but not in the case of GA101-exposed cells.

The expression levels of CD19, as well as of complement inhibitors CD46, CD55, and CD59, on RL cells were studied after 1, 2, 4, 6, and 24 hours *in vitro* exposures to GA101 or rituximab, in the presence or absence of CVF. There was no change in the CD19 expression after exposure to rituximab or GA101 (data not shown). In addition, we did not observe any upregulation of the CD46, CD55, and CD59 antigens in tumor cells exposed *in vivo* to either antibody. Although procaspase-3 was found slightly increased by Western blot analysis in the GA101-treated group in comparison with untreated or rituximab-treated mice 12 hour after exposure, we did not observe cleaved form of caspase-3 expression following these *in vivo* experiments (data not shown).

Gene expression arrays

In RL cells exposed to mAb *in vitro* for 6 hours, a total of 867 genes were induced by rituximab and 664 by GA101, including 152 genes induced by both antibodies (See Supplementary Table 1). A series of genes found to be significantly overexpressed after exposure both to rituximab and to GA101 were analysed by RT-PCR (data not shown). Among these, overexpression of EGR1 and ATF3 were confirmed in 3 independent experiments. EGR1 was increased up to 10-fold and ATF3 to 4-fold in RL cells after exposure to antibodies ($P < 0.01$). Increased expression of the corresponding proteins was also documented by immunoblotting (Fig. 6). We did not observe increase in Bax protein level expression.

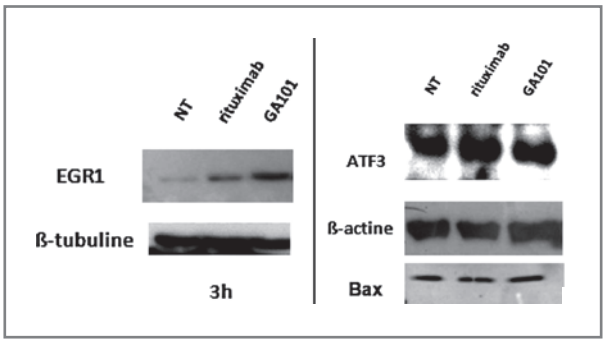

Figure 6. Effect of rituximab and GA101 on EGR1, Bax, and ATF3 expression in RL tumors. EGR1, Bax, and ATF3 protein levels were evaluated by Western blotting after exposure of RL cells to rituximab and GA101 *in vitro*.

Gene ontology pathways of the genes induced by rituximab and GA101 are presented in Supplementary Tables 2 and 3. Interleukin 12 (IL-12) biosynthesis, glucose import, and ribosome biogenesis were among the pathways most significantly enriched after exposure to rituximab. Response to biotic stimulus or parasites, immune activation, and IL-1 biosynthesis were among the pathways most significantly enriched after exposure to GA101. Several pathways were found to be enriched with both antibodies, including IL-1, IL-6, IL-13 biosynthesis as well as negative regulation of cell differentiation and osteoclast differentiation. It thus appears that the pathways activated by these 2 anti-CD20 antibodies partially overlap but differ significantly in other aspects.

Discussion

This preclinical study was initiated to compare the *in vivo* efficacy of rituximab, the first in class anti-CD20 mAb, and GA101, a novel generation CD20 antibody, in a preclinical model of human NHL. The results show the superior antitumor activity of GA101 in a model of human FL RL grown as xenografts in SCID mice, either as a single agent or in combination with cyclophosphamide, in comparison to rituximab. The effect of GA101 did not appear to involve complement, whereas the effect of rituximab in this model was at least partially complement dependent. Tolerability of GA101 with these regimens was excellent with no toxic deaths and no significant modification of body weight.

The role of complement in anti-CD20 treatment is now a matter of debate. CDC is clearly involved in the action of rituximab both *in vitro* and in preclinical mouse models (21, 22, 32–34). Manches et al. have also reported a correlation between *in vitro* sensitivity to CDC of various lymphoma subtypes and the likelihood of response to rituximab in the clinic (17). Conversely, it has been suggested that deposition of inactivated C3b on rituximab-coated cells could diminish the interaction between the Fc region and CD16 on NK cells. Our *in vivo* results using rituximab corroborate the previously reported data and support the role of complement in rituximab-mediated antitumor activity. However, we did not observe variations in the expression of the complement inhibitors CD46, CD55, or CD59 in our model. These antigens have been reported to be altered in cells exposed to antibodies or to be correlated with response to anti-CD20 antibodies (20). In the case of GA101, the role of CDC is clearly less important both *in vitro* and *in vivo* (29).

In the SCID mice model, it is not expected that a major contribution to efficacy comes from the optimized interaction of the glycoengineered Fc-part of GA101 with the murine FcγRIV receptors expressed on macrophages/monocytes. Thus, the direct induction of cell death is likely to play an important role in GA101-mediated cytotoxicity. In support of this hypothesis, we observed a greater induction of early cell death as well as higher expression of procaspase-3 and Bad protein after exposure to GA101 than after exposure to rituximab. Although the activated form of caspase-3 was not detected in our animal model euthanized 12 hours after last exposure to treatment, we observed in additional *in vitro* kinetic experiments that the cleaved-caspase-3 form was mainly detectable after 24 and 48 hours of exposure.

The signalization pathways involved in anti-CD20 antibody-mediated cytotoxicity have been explored by several groups. Bonavida and Jazirehi have reported the importance of RKIP as a central regulator of rituximab-induced cytotoxicity, regulating BclX-L (35). Leseux et al. have found that PKCζ was involved in cytotoxicity of rituximab in the RL line (36). In this study, we identified 2 novel proteins potentially involved in CD20-mediated cytotoxicity. ATF3 and EGR1 were overexpressed both after exposure to rituximab and to GA101, suggesting that they may be involved in CD20-mediated signaling. EGR1 or early growth response 1 is a zinc finger protein that has been reported to possess both oncogenic and tumor suppressor properties. Zheng et al. have shown that NFκB-induced EGR1 transcription allowed survival of prostate tumor cells, whereas other authors have suggested a proapoptotic role by induction of Bax (37, 38). ATF3, or activating transcription factor 3, is a leucine zipper protein involved in cellular stress pathways. ATF3 has been reported to behave as an oncogene in murine mammary carcinogenesis, but has also been found to be involved in apoptosis in prostate cancer (39, 40). Additional experiments are required to show whether the overexpression of these genes after exposure to anti-CD20 monoclonal antibodies is required for cytotoxicity.

In conclusion, these results show that GA101 used as a single agent or in combination with cyclophosphamide is more active than rituximab on human lymphoma RL xenografts. As expected for a Type II antibody, GA101 appears not to act through CDC, and is more potent than the Type I antibody rituximab in inducing cell death via nonclassical induction of apoptosis.

Disclosure of Potential Conflicts of Interest

S. Dalle received a research grant from Roche to Inserm.

Grant Support

This work was funded in part by a grant support from Roche to INSERM 590.

The costs of publication of this article were defrayed in part by the payment of page charges. This article must therefore be hereby marked *advertisement* in accordance with 18 U.S.C. Section 1734 solely to indicate this fact.

Received April 23, 2010; revised October 15, 2010; accepted October 27, 2010; published online January 10, 2011.

References

1. Dillman RO. Treatment of low-grade B-cell lymphoma with the monoclonal antibody rituximab. Semin Oncol 2003;30:434-47.
2. Coiffier B. Rituximab therapy in malignant lymphoma. Oncogene 2007;26:3603-13.
3. Hiddemann W, Kneba M, Dreyling M, Schmitz N, Lengfelder E, Schmits R, et al. Frontline therapy with rituximab added to the combination of cyclophosphamide, doxorubicin, vincristine, and prednisone (CHOP) significantly improves the outcome for patients with advanced-stage follicular lymphoma compared with therapy with CHOP alone: results of a prospective randomized study of the German Low-Grade Lymphoma Study Group. Blood 2005;106:3725-32.
4. Lin TS, Lucas MS, Byrd JC. Rituximab in B-cell chronic lymphocytic leukemia. Semin Oncol 2003;30:483-92.
5. Ghobrial IM, Gertz MA, Fonseca R. Waldenstrom macroglobulinaemia. Lancet Oncol 2003;4:679-85.
6. Colombat P, Salles G, Brousse N, Eftekhari P, Soubeyran P, Delwail V, et al. Rituximab (anti-CD20 monoclonal antibody) as single first-line therapy for patients with follicular lymphoma with a low tumor burden: clinical and molecular evaluation. Blood 2001;97:101-6.
7. Hainsworth JD, Litchy S, Burris HA 3rd, Scullin DC Jr, Corso SW, Yardley DA, et al. Rituximab as first-line and maintenance therapy for patients with indolent non-Hodgkin's lymphoma. J Clin Oncol 2002;20:4261-7.
8. McLaughlin P, Grillo-López AJ, Link BK, Levy R, Czuczman MS, Williams ME, et al. Rituximab chimeric anti-CD20 monoclonal antibody therapy for relapsed indolent lymphoma: half of patients respond to a four-dose treatment program. J Clin Oncol 1998;16:2825-33.
9. Davis TA, Grillo-Lopez AJ, White CA, McLaughlin P, Czuczman MS, Link BK, et al. Rituximab anti-CD20 monoclonal antibody therapy in non-Hodgkin's lymphoma: safety and efficacy of re-treatment. J Clin Oncol 2000;18:3135-43.
10. Lemieux B, Bouafia F, Thieblemont C, Hequet O, Arnaud P, Tartas S, et al. Second treatment with rituximab in B-cell non-Hodgkin's lymphoma: efficacy and toxicity on 41 patients treated at CHU-Lyon Sud. Hematol J 2004;5:467-71.
11. Ghielmini M, Schmitz SF, Cogliatti SB, Pichert G, Hummerjohann J, Waltzer U, et al. Prolonged treatment with rituximab in patients with follicular lymphoma significantly increases event-free survival and response duration compared with the standard weekly × 4 schedule. Blood 2004;103:4416-23.
12. Hainsworth JD, Litchy S, Shaffer DW, Lackey VL, Grimaldi M, Greco FA. Maximizing therapeutic benefit of rituximab: maintenance therapy versus re-treatment at progression in patients with indolent non-Hodgkin's lymphoma—a randomized phase II trial of the Minnie Pearl Cancer Research Network. J Clin Oncol 2005;23:1088-95.
13. Smith MR. Rituximab (monoclonal anti-CD20 antibody): mechanisms of action and resistance. Oncogene 2003;22:7359-68.
14. Maloney DG. Immunotherapy for non-Hodgkin's lymphoma: monoclonal antibodies and vaccines. J Clin Oncol 2005;23:6421-8.
15. Dalle S, Thieblemont C, Thomas L, Dumontet C. Monoclonal antibodies in clinical oncology. Anticancer Agents Med Chem 2008;8:523-32.
16. Anderson DR, Grillo-Lopez A, Varns C, Chambers KS, Hanna N. Targeted anti-cancer therapy using rituximab, a chimaeric anti-CD20 antibody (IDEC-C2B8) in the treatment of non-Hodgkin's B-cell lymphoma. Biochem Soc Trans 1997;25:705-8.
17. Manches O, Lui G, Chaperot L, Gressin R, Molens JP, Jacob MC, et al. In vitro mechanisms of action of rituximab on primary non-Hodgkin lymphomas. Blood 2003;101:949-54.
18. Golay J, Lazzari M, Facchinetti V, Bernasconi S, Borleri G Barbui T, et al. CD20 levels determine the in vitro susceptibility to rituximab and complement of B-cell chronic lymphocytic leukemia: further regulation by CD55 and CD59. Blood 2001;98:3383-9.
19. Bellosillo B, Villamor N, López-Guillermo A, Marcé S, Esteve J, Campo E, et al. Complement-mediated cell death induced by rituximab in B-cell lymphoproliferative disorders is mediated in vitro by a caspase-independent mechanism involving the generation of reactive oxygen species. Blood 2001;98:2771-7.
20. Golay J, Zaffaroni L, Vaccari T, et al. Biologic response of B lymphoma cells to anti-CD20 monoclonal antibody rituximab in vitro: CD55 and CD59 regulate complement-mediated cell lysis. Blood 2000;95:3900-8.
21. Golay J, Cittera E, Di Gaetano N, et al. The role of complement in the therapeutic activity of rituximab in a murine B lymphoma model homing in lymph nodes. Hematological 2006;91:176-83.
22. Di Gaetano N, Cittera E, Nota R, et al. Complement activation determines the therapeutic activity of rituximab in vivo. J Immunol 2003;171:1581-7.
23. Weng WK, Levy R. Expression of complement inhibitors CD46, CD55, and CD59 on tumor cells does not predict clinical outcome after rituximab treatment in follicular non-Hodgkin lymphoma. Blood 2001;98:1352-7.
24. Shan D, Ledbetter JA, Press OW. Signaling events involved in anti-CD20-induced apoptosis of malignant human B cells. Cancer Immunol Immunother 2000;48:673-83.
25. Chan HT, Hughes D, French RR, Tutt AL, Walshe CA, Teeling JL, et al. CD20-induced lymphoma cell death is independent of both caspases and its redistribution into triton X-100 insoluble membrane rafts. Cancer Res 2003;63:5480-9.
26. Beers SA, Chan CH, James S, French RR, Attfield KE, Brennan CM, et al. Type II (tositumomab) anti-CD20 monoclonal antibody out performs Type I (rituximab-like) reagents in B-cell depletion regardless of complement activation. Blood 2008.
27. Clynes RA, Towers TL, Presta LG, Ravetch JV. Inhibitory Fc receptors modulate in vivo cytotoxicity against tumor targets. Nat Med 2000;6:443-6.
28. Bonavida B. Rituximab-induced inhibition of antiapoptotic cell survival pathways: implications in chemo/immunoresistance, rituximab unresponsiveness, prognostic and novel therapeutic interventions. Oncogene 2007;26:3629-36.
29. Mössner E, Brünker P, Moser S, Püntener U, Schmidt C, Herter S, et al. Increasing the efficacy of CD20 antibody therapy through the engineering of a new type II anti-CD20 antibody with enhanced direct- and immune effector cell-mediated B-cell cytotoxicity. Blood 2010;115:4393–402.
30. Dalle S, Dupire S, Brunet-Manquat S, Reslan L, Plesa A, Dumontet C. In vivo model of follicular lymphoma resistant to rituximab. Clin Cancer Res 2009;15:851-7.
31. Bolstad BM, Irizarry RA, Astrand M, Speed TP. A comparison of normalization methods for high density oligonucleotide array data based on variance and bias. Bioinformatics 2003;19:185-93.
32. Cragg MS, Morgan SM, Chan HT, et al. Complement-mediated lysis by anti-CD20 mAb correlates with segregation into lipid rafts. Blood 2003;101:1045-52.
33. Daniel D, Yang B, Lawrence DA, Totpal K, Balter I, Lee WP, et al. Cooperation of the proapoptotic receptor agonist rhApo2L/TRAIL with the CD20 antibody rituximab against non-Hodgkin lymphoma xenografts. Blood 2007;110:4037-46.
34. Cittera E, Leidi M, Buracchi C, Pasqualini F, Sozzani S, Vecchi A, et al. The CCL3 family of chemokines and innate immunity cooperate in vivo in the eradication of an established lymphoma xenograft by rituximab. J Immunol 2007;178:6616-23.
35. Jazirehi AR, Bonavida B. Cellular and molecular signal transduction pathways modulated by rituximab (rituxan, anti-CD20 mAb) in non-Hodgkin's lymphoma: implications in chemosensitization and therapeutic intervention. Oncogene 2005;24:2121-43.
36. Leseux L, Laurent G, Laurent C, Rigo M, Blanc A, Olive D, Bezombes C. PKC zeta mTOR pathway: a newtarget for rituximab therapy in follicular lymphoma. Blood 2008;111:285–91.
37. Zheng C, Ren Z, Wang H, Zhang W, Kalvakolanu DV, Tian Z, et al. E2F1 Induces tumor cell survival via nuclear factor-kappaB-dependent induction of EGR1 transcription in prostate cancer cells. Cancer Res 2009;69:2324-31.
38. Zagurovskaya M, Shareef MM, Das A, et al. EGR-1 forms a complex with YAP-1 and upregulates Bax expression in irradiated prostate carcinoma cells. Oncogene 2009;28:1121-31.
39. Wang A, Arantes S, Yan L, Kiguchi K, McArthur MJ, Sahin A, et al. The transcription factor ATF3 acts as an oncogene in mouse mammary tumorigenesis. BMC Cancer 2008;8:268.
40. Huang X, Li X, Guo B. KLF6 induces apoptosis in prostate cancer cells through up-regulation of ATF3. J Biol Chem 2008;283:29795-801.

Molecular Cancer Therapeutics

Preclinical Studies on the Mechanism of Action and the Anti-Lymphoma Activity of the Novel Anti-CD20 Antibody GA101

Stephane Dalle, Lina Reslan, Timothee Besseyre de Horts, et al.

Mol Cancer Ther 2011;10:178-185.